



High Strength Dual Phase Steels and Flow Curve Modeling Approach

Sawitree Sodjit, Vitoon Uthaisangsuk^{*}

Department of Mechanical Engineering
Faculty of Engineering, King Mongkut's University Technology Thonburi, Thailand 10140

^{*}Corresponding Author: Tel: 02 470 9274, Fax: 02 470 9111

E-mail: vitoon.uth@kmutt.ac.th

Abstract

Dual Phase (DP) steels are an important advanced high strength steel, which have been widely used in the automotive industry for vehicle components requiring light weight and safety. A microstructure of DP steel generally consists of martensitic islands embedded in ferritic matrix. DP steel in this investigation was produced by using two commercial hot-rolled strips as the raw material. Different intercritical temperatures were considered during annealing process in order to generate different martensite phase fractions. Initially, Thermo-Calc calculation was performed to find a proper temperature range of the austenite-ferrite two-phase region for the intercritical annealing process. After the annealing, microstructures of the produced DP steels were characterized by Light Optical Microscope (LOM) and Scanning Electron Microscope (SEM). It was found that the microstructures of the DP steels contain globular and irregular martensite surrounded by ferritic matrix. Ferrite-martensite morphology and martensite phase fraction (MPF) play the most significant role on the mechanical properties of DP steel. Obviously, yield and ultimate tensile strength of DP steel were increased with increasing MPF, but the elongation was reduced. Additionally, micromechanical FE modeling was carried out for predicting flow curves of both DP steels. 2D Representative Volume Element (RVE) was prepared based on micrographs of real dual phase microstructures. A physically based model was applied to describe the stress-strain behaviour of individual phases in DP steel. The model also takes the grain boundary dislocation (GBD) density into account, which has contribution to both an increase in forest dislocations and a building up of back stresses. Finally, calculated stress-strain curves were compared with experimental stress-strain curves determined from tensile test.

Keywords: Dual Phase Steel, Intercritical Annealing, Flow curve, Microstructure

1. Introduction

In recent years, the industries have paid more attention to environmental impact of their

production, for example CO₂ gas emission that principally involved in the global warming problem. Therefore, reduction of energy



consumption in every industrial section is indispensable. In order to meet this demand, optimization of well-known materials and developing new materials with a high ratio of strength to density and a good suitability for metal forming operation are still progressed [1, 2].

Dual phase (DP) steels are one of the important advanced high strength steel (AHSS) products developed for the automotive industry, in which steel grade exhibiting high strength and good formability is required so that weight of vehicle can be reduced for fuel saving purpose. Microstructures of the DP steel contain harder martensitic phase from 5 to 35 percent in a relatively soft and ductile ferrite matrix. Thus, DP steels have characteristic mechanical properties which include low yield strength and high ultimate tensile strength as compared with conventional low-carbon steel. The weight of products made from this steel can be considerably decreased, but their mechanical properties remain the same or are even improved. Furthermore, DP steel also show a high work-hardening rate in the early stage of plastic deformation and a good ductility during forming process relative to their strength [3]. To optimize a combination of strength and formability of DP steel, an accurate description of material properties using a physically based model is necessary. By performing FE simulations of industrial forming processes, the microstructure of used high strength steels has not been considered at present, which essentially is the most important factor influencing the mechanical properties of such multiphase steels [4]. Within this research, DP

steels having different martensite phase fractions (MPF) were prepared from hot-rolled steels with two chemical compositions by intercritical annealing process. Metallographic investigation and tensile tests were carried out for characterizing the produced DP steels. Subsequently, micrographs of the steels taken from light optical microscope were applied for generating 2D Representative Volume Element (RVE). Microstructure based RVE simulations were afterwards conducted in order to predict the stress-strain behaviour of each investigated DP steel. Individual material models based on the dislocation theory were used to describe the flow curves of both ferritic and martensitic phases in the simulations [5]. It was found that differences in microstructural characteristics depending on alloying elements and annealing schedules significantly influence mechanical properties of the DP steels. To verify the modeled flow curves and the FE results comparisons between experimental and numerical stress-strain responses were done. The purpose of this research is to better understand the deformation and fracture behaviour of DP steels with respect to local stress-strain distributions in their microstructure.

2. Experimental procedure

2.1. Materials

Materials used in this work are low carbon steels of the grade JIS G3101 SS400 (will be called S1 later) and JIS G3106 SM 490 (will be called S2 later). The chemical compositions of both steel grades were determined using vacuum emission spectroscopy as shown in Table 1. The steel S2 has higher carbon, silicon, and manganese



content than the steel S1, but other elements are similar. Carbon increases martensite phase fraction during quenching by reducing the critical cooling rate. Manganese was added in order to promote adequate hardenability. Silicon was added with the purpose of increasing the strength of the solid solution and inhibiting precipitation of cementite at the ferrite-martensite interface during the water cooling stage [6]. Firstly, as-received hot-rolled steel strips with a thickness of 2.6 mm were cut to rectangular dimension of 100x300 mm. Then, the steel sheets were pickled by a solution of 20% HCl in water at the temperature of 80°C. The steel sheets were rolled using a twin rolling mill at room temperature in order to obtain a final thickness of 1 mm. This thickness reduction is approximately according to a cold-rolling degree of 45%. After that, specimens for tensile test were prepared parallel to the rolling direction.

Table 1 Chemical composition in weight percent of the investigated steels

Material	C	Si	S	P	Mn	Ni	Cu
S1	0.112	0.018	0.013	0.015	0.519	0.065	0.044
S2	0.173	0.235	0.010	0.016	0.809	0.009	0.025

Afterwards, heat treatment was carried out for the samples to obtain steel with dual phase microstructure containing different martensitic phase fraction. Hereby, the samples were quenched by water from different intercritical annealing temperatures (IAT) to room temperature. The heat treatment process was done in a salt bath furnace, for which a salt values could be calculated directly as an extensometer was used. The reproducibility of the determined stress-strain curves was

composition of the mixture of 78% BaCl₂ and 22% NaCl was used. The intercritical temperatures in the experiment were initially calculated by means of the software "Thermo-Calc". The samples of material S1 were heated to different IAT temperatures of 735, 750, 785, and 800°C between the A_{C1} and A_{C3} temperature in order to produce DP microstructures having MPF of 10, 20, 30 and 40%, respectively. By the same manner, the samples of material S2 were heated to the temperatures of 750 and 790°C for achieving DP steels with MPF of 30 and 50%. The holding time after reaching each intercritical temperature was 5 min. Finally, the samples were quenched in cold water (the temperature was about 10°C).

2.2 Mechanical testing

Tensile test according to the ASTM E8M standard test methods for tension testing of metallic materials was performed for the heat-treated specimens. Here, the sub-size tensile sample with a nominal gauge length of 25.4 mm and nominal width of 6.4 mm was used. These specimens were elongated under uniaxial condition on a universal testing machine, which is equipped with an automatic controller using displacement control mode. A cross-head speed of 0.04 mm/s that is equal to a quasi-static strain rate of 0.002 s⁻¹ was applied. Three repeated specimens for each DP steels with different MPFs were tested. During the tests, force and displacement of the sample were recorded. From these data, conventional stress and strain acceptable and necking was mostly observed inside the gauge length for all samples. The ultimate tensile strength and uniform elongation

are presented together with the respective volume fraction and intercritical temperature in Table 2 for both investigated DP steels. Obviously, the DP steel of grade S2 exhibited higher tensile strength than the DP steel of grade S1 when considering the same volume fraction of martensite. This higher strength could be due to the martensitic phase that is harder in the DP steel S2 with higher carbon content. However, the higher hardness value of martensite certainly led to a lower uniform elongation.

Table 2 Mechanical properties of the investigated DP steels

Material	IAT (°C)	Volume fraction (%)	UTS (MPa)	Uniform elongation (%)
S1	735	10	528	21.5
	750	20	601	22.6
	785	30	657	21.9
	800	40	708	20.8
S2	750	30	794	18.0
	770	40	925	16.0
	790	50	1174	15.7

2.3 Microstructure investigation

Samples for metallographic analysis were prepared from the specimens after tensile

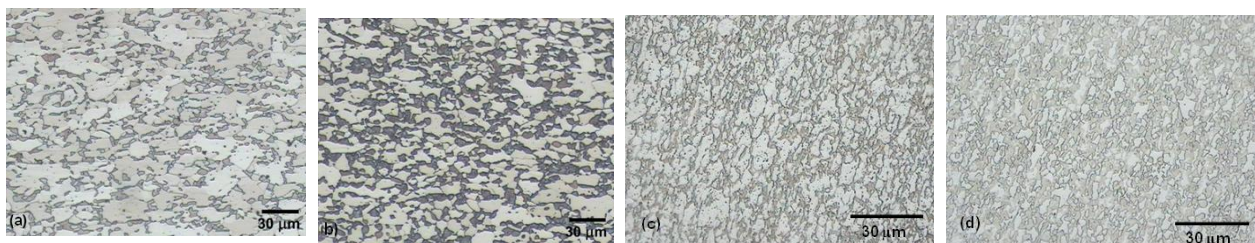


Fig. 1 Optical micrographs of DP steel S1 with (a) MPF=20% (b) MPF=40% and optical micrographs of DP steel S2 with (c) MPF=30% (d) MPF=50%

It was found that size of martensite islands in the DP steel S1 are larger than in the DP steel S2. Since ferritic grains in the DP steel

test for the region undergoing minimum deformation. In this case, it is the area of the sample shoulder. The sample were grounded using silicon carbide paper with a grit size of 240, 400, 600, 1000 and 1200 in sequence, and were then polished with 1 μm and 0.03 μm alumina, respectively. After polishing, the specimens were pre-etched with a 2% Nital solution (2 ml HNO₃ in 98 ml ethanol) for 3-5 seconds and followed by a 5% Na₂S₂O₅ (5 g Na₂S₂O₅ in 95 ml distilled water) about 10-15 seconds for tint-etching [5]. The volume fractions and grain sizes of each specimen were determined using MSQ image analysis. The measurement of the volume fraction was based on area percent. Fig. 1 illustrates micrographs from light optical microscope for the DP steel S1 with the MPF of 20% and 40% and the DP steel S2 with the MPF of 30% and 50%. In the microstructures, the bright gray zones are ferritic phase and the dark gray regions are martensitic islands. Grain sizes of ferritic phase in the DP steel S1 and S2 were measured using the lineal intercept method and were averaged, for example, for the DP steels with a MPF of 30% to be about 13 and 5 μm, respectively.

S1 are larger, there are less grain boundaries in the microstructures. Thus, martensites in the DP steel S1 are not distributed to overall area of the

microstructure, but rather allocated as a large island. In contrast, martensitic islands in the DP steel S2 are finely dispersed in the entire microstructure along the ferritic grain boundaries.

3.1 Representative Volume Element

The behavior of multiphase steels has been normally described using continuum mechanics on the so-called macroscale. On this scale the entire material is treated as a continuum, whereas on the microstructure level, or the so-called mesoscale, the material is clearly discontinuous because of its multiphase character. Thus, the assumption of homogeneity and continuity is valid on the macro-scale only. The determination of macroscopic mechanical properties can be interpreted as an averaging over the microstructure volume elements. Such an element is called a Representative Volume Element (RVE). A RVE exhibits both phase composition and microstructural arrangement. RVE can be identified easily as a cut-out of the macroscopic material. It needs to be big enough to represent the most important microstructural features of the investigated material. Besides, for the determination of macroscopic properties, an investigation using RVE provides information about stress and strain distribution of each

constituent phase and its contribution to the overall strength of material. By defining a RVE, several assumptions for the complexity in the form and distribution of the phases are necessary. In case of a two phase microstructure with spherical second phase inclusions in a surrounding matrix, the simplest assumption is that the second phase distribution is homogenous, periodic and globular. In general, three steps have to be considered for the calculation of the overall strain hardening behavior of dual phase steel by using RVE method:

- (a) Geometric definition of the RVE, which embodies the essential features of the microstructure
- (b) Constitutive description of the mechanical behavior of each phase
- (c) Homogenization strategy for macroscopic mechanical behavior

To what extent the RVE can describe behavior of the microstructure depends in such a way on how accurately the RVE captures the morphological features of the actual microstructure. Calculation accuracy and model simplifications for easy and fast calculations are oppositional requirements in this context [7].

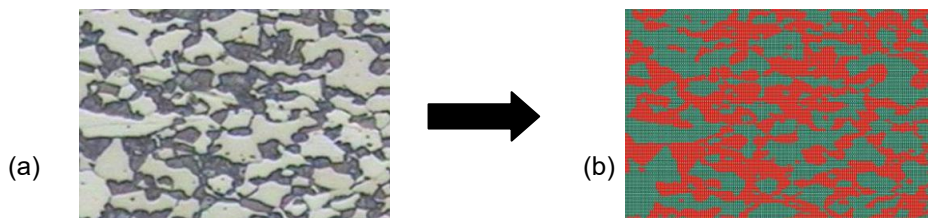


Fig. 2 (a) Original micrograph of an investigated DP microstructure and (b) 2D RVE model generated from the microstructure alongside with 160x160 elements and MPF of 40%

In this work, 2D RVE simulation was carried out, for which precise model and material properties must be prepared. At first, a

micrograph of real microstructure was converted to a 2D FEM model. By this manner, microstructural morphology as well as amount of



martensite and ferrite could be considered. A 2D RVE model generated from real DP microstructure is shown in Fig. 2, which was used as a 2D model for FE calculation. The FE simulations were performed using ABAQUS and the flow behaviors of DP steels were afterwards determined.

3.2 Microstructure based flow curve behaviour

3.2.1 Model

Flow curves of individual phases for ferrite and martensite at room temperature was described based on the dislocation theory [8]. According to these works the effective stress-strain can be described as

$$\sigma = \sigma_0 + \Delta\sigma + \alpha \cdot M \cdot \mu \cdot \sqrt{b} \cdot \sqrt{\frac{1 - \exp(-Mk_r \varepsilon)}{k_r \cdot L}} \quad (1)$$

where σ is the flow stress at a true strain of ε . The descriptions of each term are given below and the values for each parameter were taken from earlier works [9]. The first term σ_0 represents the Peierls stress and effects of elements in solid solution as followed.

$$\begin{aligned} \sigma_0 \text{ (in MPa)} = & 77 + 750 (\%P) + 60 (\%Si) + 80 \\ & (\%Cu) + 45 (\%Ni) + 60 (\%Cr) + 80 (\%Mn) + \\ & 11(\%Mo) + 5000 (\%N_{ss}) \end{aligned} \quad (2)$$

The second term $\Delta\sigma$ provides material strengthening by precipitation or carbon content in solution. In case of ferrite it is given by

$$\Delta\sigma \text{ (in MPa)} = 5000 * (\%C_{ss}^f) \quad (3)$$

While for martensite it is given by

$$\Delta\sigma \text{ (in MPa)} = 3065 * (\%C_{ss}^m) - 161 \quad (4)$$

The third term comprises of the effects of dislocation strengthening as well as work softening due to recovery. α is a constant having a value of 0.33. M is the Taylor factor, and a value of 3 was utilized in this study. μ is the shear modulus and a value of 80000 MPa was applied. b is the Burger's vector and a value of $2.5 \cdot 10^{-10}$ m was taken. k_r is the recovery rate. In case of ferrite a value of $10^{-5}/d_\alpha$ was in use, whereas d_α refers to the ferritic grain size. L is the dislocation mean free path [8,10]. For ferrite, it is equal to the ferritic grain size d_α , while for martensite the values L and k_r were used as fitting parameters, as shown in Table 3.

Table 3 Model parameters for calculating flow curves of the investigated DP steels

Material	parameter	ferrite	martensite
S1	k_r	$10^{-5}/d_\alpha$	35
	L	$0.4 \times 10^{-5} / k_r$	1.9×10^{-7}
S2	k_r	$10^{-5}/d_\alpha$	2
	L	$0.4 \times 10^{-5} / k_r$	0.15×10^{-7}

On the one hand, the dislocations stored in the vicinity of the boundary will contribute to forest hardening causing an isotropic hardening. On the other hand, these dislocations will lead to the building up of back stresses giving a kinematic hardening. At small strains, grain boundaries act as perfectly barriers of dislocations. Thus, dislocations are stopped at the grain boundaries causing a back stress. Both the dislocation accumulation at the grain boundaries in ferrite and the incompatibility between the martensite islands and the ferrite matrix contribute to the polarized stress. The net polarized stress arising

from long range back stress can be expressed in term of the resulting backstress (σ_s) [11]:

$$\sigma_s = \left[\frac{M\mu b n^*}{d_\alpha} \exp\left(\frac{-\lambda \varepsilon}{bn^*}\right) \left(1 - \exp\left(\frac{-\lambda \varepsilon}{bn^*}\right)\right) \right] \quad (5)$$

It was assumed that grain boundary efficiency for generating back stresses and for dislocation storage are dictated by the same critical number of dislocations at the boundary n^* . λ is the mean spacing between slip lines at the grain boundaries. For the flow curve of ferritic phase this kinematic hardening behaviour was additionally taken into account by Eq. (5). The values of n^* and λ were used as fitting parameters [12].

3.2.2 Flow curves of individual single phase

To obtain the flow curves for ferrite and martensite, approaches [8] as discussed in the previous section were applied. Modeled flow curves for ferrite in DP steel S1 and S2 with different MPF values are depicted in Fig. 3 and Fig. 4, respectively. Averaged grain size of ferrite for each DP compositions was also given. Small discrepancies between flow curves of the ferrite in DP steels annealed at various temperatures were found due to the different observed grain sizes. A bit higher yield strength and strain hardening are noticed for the DP microstructures containing ferritic phase that exhibits smaller grain size. Finer ferritic grain occurred in the microstructure with higher martensite fraction. A saturation of the ferrite flow curves at higher strains can be seen in case of the DP steels S2.

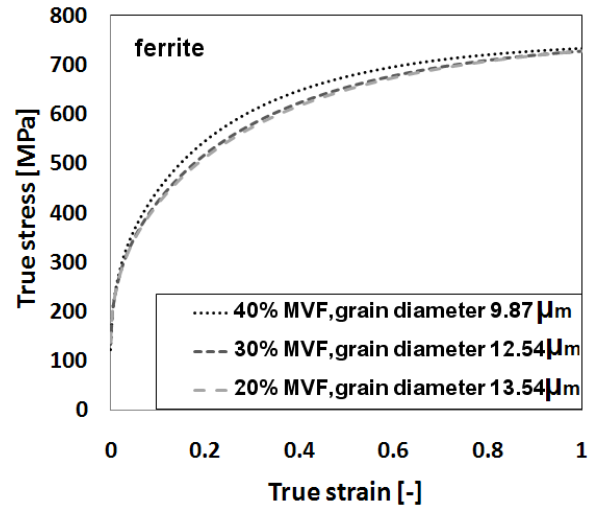


Fig. 3 Modeled flow curves for ferrite in the DP steel S1 having different MPF values and ferritic grain sizes

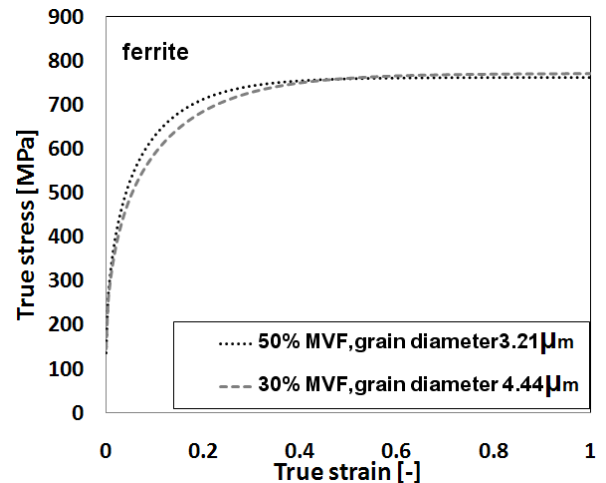


Fig. 4 Modeled flow curves for ferrite in DP steels S2 having different MPF values and ferritic grain sizes

Modeled martensite flow curves for the DP steel S1 and S2 are shown in Fig. 5 and Fig. 6, respectively. Deviations of the flow curves of martensite phases in the DP steels annealed at various temperatures are apparent when comparing with the ferrite flow curves. The martensite presented much higher stresses than the ferrite in all DP steels. Furthermore, all martensite flow curves showed saturated stress characteristics at small strains, and the maximum stresses were reached much earlier in

case of the DP steels S2. The stress-strain development of martensite clearly indicates its brittle behaviour. The martensites in the DP steels S2 are more brittle than in the DP steel S1. It has been established that martensites in the DP steel S1 should be able to sustain more deformation before failure.

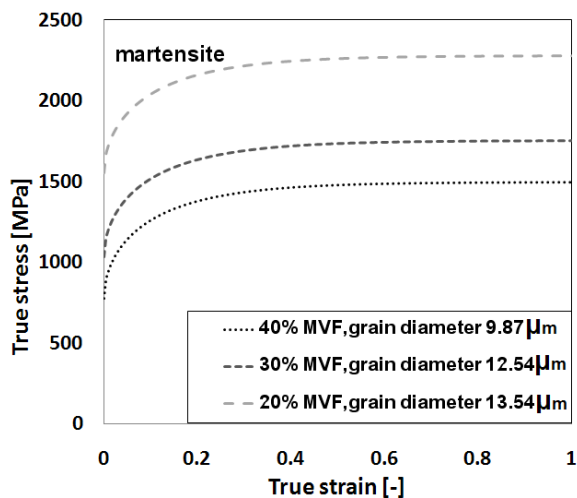


Fig. 5 Modeled flow curves for martensite in the DP steel S1 having different MPF values and ferritic grain sizes

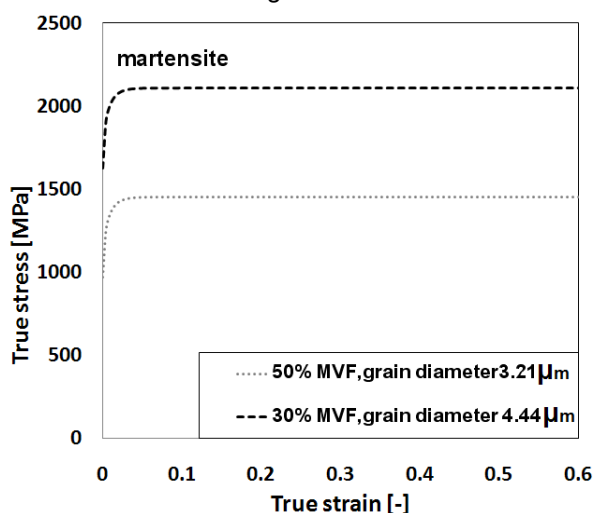


Fig. 6 Modeled flow curves for martensite in DP steels S2 having different MPF values and ferritic grain sizes

Thus, local stress-strain distribution in the microstructure of the DP steel S1 should be more homogeneous and a higher material

ductility can be then expected. In DP steels with lower MPF value, carbon content in martensite is higher that significantly led to both much increased yield and maximum stresses of the martensite.

4. Results

4.1 Comparisons of experimental and numerical flow curves

FE simulations for the 2D RVE model were performed under uniaxial straining condition. From the simulations, overall stress-strain curves were determined for different DP microstructures. These results were compared with experimental stress-strain curves from quasi-static tensile tests for the corresponding DP structures. The comparisons are shown in Fig. 7 and Fig. 8 for the DP steel S1 and S2 containing different martensite contents, respectively. In case of the DP steel S1 flow curves from FE simulations agreed well with experimental curves, especially with regard to strain hardening behaviour. For the DP steel S2, the results of flow curve prediction were very accurate in case of 30% MPF. The predicted flow curve of the DP steel S2 with 50% MPF was underestimated, particularly at higher strain value. However, the strain hardening rate could be correctly described. It should be noted that when a difference between the flow curve of ferrite and martensite is remarkable because of high carbon content in martensite, an underestimated stress-strain response could be calculated from the RVE simulation.

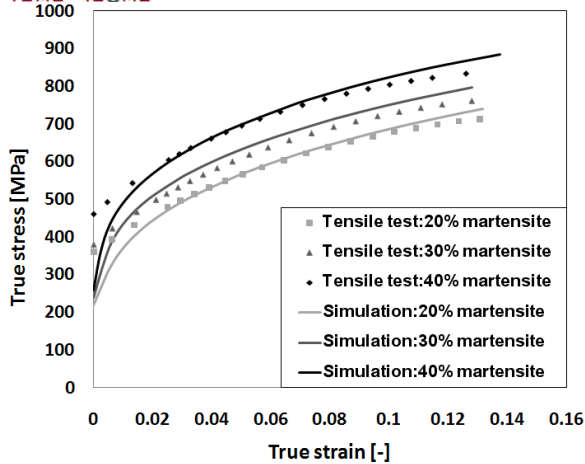


Fig. 7 Comparison between experimental and numerical flow curves for the DP steel S1 with 20, 30, and 40% MPF

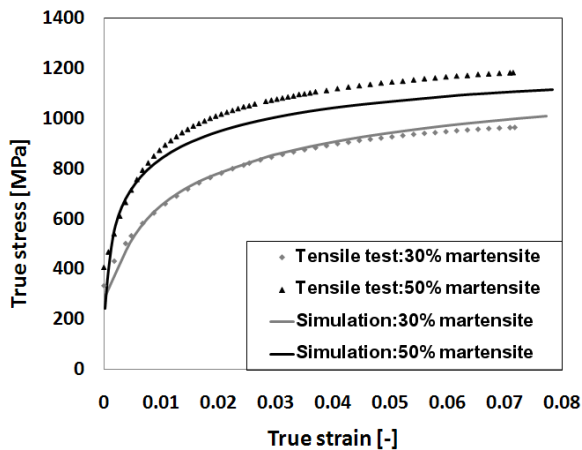


Fig. 8 Comparison between experimental and numerical flow curves for the DP steel S2 with 30 and 50% MPF

4.2 Local stress-strain distribution

In the 2D RVE model real morphologies and all microstructural constituents of DP steel were considered on the micro-level. Evolution of local stress and strain in the DP microstructure was obtained from the RVE simulations. Distribution of equivalent von Mises stress in the microstructure of the DP steel S1 and S2 consisting of 30% martensite phase fraction after a macroscopic uniaxial tensile deformation of 10% is shown in Fig. 9(a) and 9(b), respectively. From RVE simulations for the DP steel S2 it was

noticed that higher stress values mostly developed along the interfaces between ferrite and martensite. The distribution of stress is more homogeneous due to the structure with finely dispersed martensite islands. Plastic deformation could be observed in the form of localized banding occurring on the direction of 45° to the tensile loading direction, as depicted in Figure 10. Since the DP steel S1 exhibits microstructure containing large martensite islands, the individual martensite regions locates broader from each other surrounding by large ferritic area. In such structure, strain could be more extended in the softer ferritic zone and the localization is regular. In contrast to the DP steel S2, strain development was restricted due to small martensite particles. Therefore, short interrupted shear bands were found in the DP steel S1, but long continuously localized bands appeared in the DP steel S2. The localization or shear bands occurred in the microstructure during the deformation strongly depends on the martensite morphology. Although, higher elongation of the DP steel S1 was also because of the properties of martensite, which showed lower strength and less brittle manner.

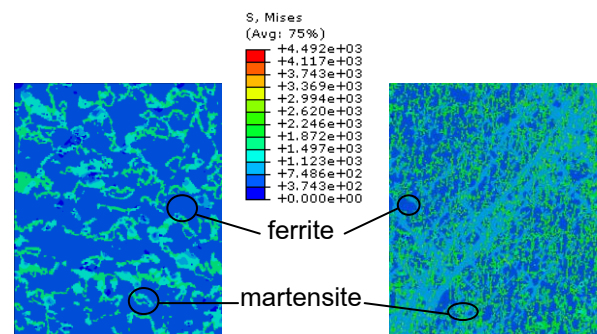


Fig. 9 Local stress distribution in 2D RVE of the DP microstructure S1 (a) and S2 (b) with a MPF of 30%

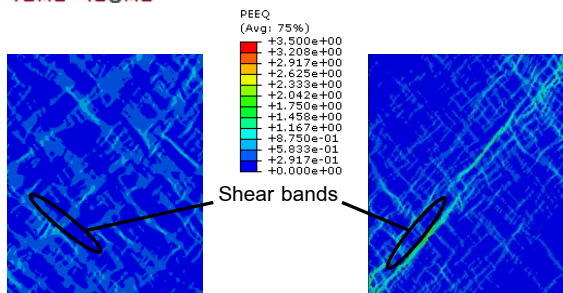


Fig. 10 Local strain distribution in 2D RVE of the DP microstructure S1 (a) and S2 (b) with a MPF of 30%

5. Conclusion

Dual phase steel shows an excellent combination between strength and ductility due to the coexistence of harder and softer phase in their microstructure. In this work, different intercritical temperatures were applied during annealing process in order to generate DP microstructure containing different martensite phase fractions between 10 to 50%. After the annealing, microstructures of the produced DP steels were characterized by LOM and tensile test was carried out. It was found that the microstructures of DP steel contain globular and irregular martensite surrounded by ferrite matrix. Yield and ultimate tensile strength of the DP steels were increased with increasing MPF, but the elongation was reduced. In addition, a microstructure based FE modeling was performed to predict flow curves of the investigated DP steels. 2D RVE was generated using real microstructure images and simulations were carried out under uniaxial tensile deformation. The results regarding the prediction of stress-strain responses were acceptable. The modeled flow curves for martensite showed very high strain hardening at the beginning and then reached a maximum constant stress. The DP steel containing higher carbon content has a

structure with harder martensite resulting in overall higher strength but decreased ductility. Mechanical properties of DP steel are also influenced by morphology of the dispersed martensitic phase. The modeling approach can be further developed and used for describing deformation and failure behaviour of multiphase steels.

6. Acknowledgement

This research work has been financially supported by the National Metal and Materials Technology Center, Thailand (MTEC).

7. References

- [1] M. J. Lee. (2005). *Advanced High Strength Steel Technology in the Ford500 and Freestyle*, Great designs in steels, Semina 2005.
- [2] Rashid, M.S. (1981). *Dual Phase Steels*, Ann. Rev. Mater. Sci. November 1981, pp. 245-266
- [3] World Auto Steel, 2009, *Advanced High Strength Steel (AHSS) Application Guidelines*, URL: [http:// www.worldautosteel.org](http://www.worldautosteel.org) access on 15/03/2009
- [4] Kyong Su Park, Kyung-Tae Park b, Duk Lak Lee c, Chong Soo Lee, (2007), *Effect of heat treatment path on the cold formability of drawn dual-phase steels*, (2007) pp.1135–1138
- [5] Micromechanical modeling of a dual phase steel, Technische universiteit eindhoven, *Annual Report 2007*
- [6] Barbara Maffei, Walter Salvatore, Renzo Valentini, (2007), *Dual-phase steel rebars for high-ductile r.c.structure, Part 1: Microstructural and mechanical characterization of steel rebars*, *Engineering Structures*, (2007) pp.3325-3332



- [7] F. Albbasi, *Micromechanical modeling of dual phase steels*, PhD Thesis, McGill University, Montral, Canada, 2004
- [8] R.M. Rodriguez, I. Gutierrez, (2003). *Unified formulation to predict the tensile curves of steels with different microstructures*, vol 426-432, pp.4525-4530
- [9] O. Bouaziz, P. Buessler, (2002). *Mechanical behavior of multiphase materials: An intermediate mixture law without fitting parameter*, La revue de metallurgie-CIT 99, (2002), pp.71-77.
- [10] V. Uthaisangasuk, U. Prah, W. Bleck, *Micromechanical modelling of damage behaviour of multiphase steels*, Computational Materials Science 43 (2008) ,pp.27-35.
- [11] M. Delince, Y. Brchet, J.D. Embury, M.G.D. Geers, P.J. Jacques, T. Pardoen, (2007). *Structure–property optimization of ultrafine-grained dual-phase steels using a microstructure-based strain hardening model*, vol.55, 2007, pp.2337–2350
- [12] C.W. Sinclair, W.J. Poole and Y. Brchet, (2006). *A model for the grain size dependent work hardening of copper*, Scripta Materialia, 2006, pp.739-742